Electronic Supplementary Material (ESI) for Nanoscale.
This journal is © The Royal Society of Chemistry 2015

Supplementary Information

Self-assembly of like-charged nanoparticles into microscopic crystals

Pramod P. Pillai,[a,b] Bartlomiej Kowalczyk,*[,a,c] and Bartosz A. Grzybowski*[,d]

[a]Department of Chemistry and Department of Chemical Engineering, Northwestern University, 2145 Sheridan Road, Evanston, Illinois

[b]Department of Chemistry, Indian Institute of Science Education and Research (IISER) Pune, Dr. Homi Bhabha Road, Pashan, Pune, 411008, India

[c]3M Purification Inc. 400 Research Parkway, Meriden, CT 064503, USA.

[d]IBS Center for Soft and Living Matter and the Department of Chemistry, Ulsan National Institute of Science and Technology (UNIST), Ulsan, South Korea

*Correspondence to: grzybor72@unist.ac.kr, bkowalczyk@mmm.com

---

Part 1. Materials and Methods.

a. Synthesis of Au Nanoparticles. Dodecylamine (DDA)-coated Au nanoparticles were prepared according to a modified literature procedure[S1]. We used $HAuCl_4 \cdot 3H_2O$ instead of $AuCl_3$ and obtained AuDDA nanoparticles of average diameters 4.2 ± 0.5 nm, 5.5 ± 0.5 nm, 8.0 ± 0.5 nm, 9.5 ± 0.5 nm, and 11.5 ± 0.5 nm. The average diameters of the nanoparticles were estimated based on TEM images of at least 200 NPs of each size. Au NPs were functionalized with a mixture of N,N,N-trimethyl(11-mercaptoundecyl)ammonium chloride (TMA) and 11-mercaptoundecanoic acid (MUA) via a ligand exchange reaction. All ultrapure-grade thiols were obtained from ProChimia Surfaces, Poland (www.prochimia.com) and used as received. Dodecyl amine (DDA) used to stabilize the NPs prior to ligand exchange reaction was purchased from Aldrich. All reagents were used as received.

b. Ligand exchange reaction. A toluene solution of DDA-capped Au NPs (20 ml, 150 μmol) was quenched with 50 ml of methanol to give a black precipitate. The precipitate was washed with methanol (50 ml), and dissolved in toluene (20 ml), to which a freshly prepared solution of MUA and TMA in 10 ml of CH_2Cl_2 was added. The molar ratios of thiols MUA:TMA (α_{soln}) used were 2, 3 and 9. The thiols were used in large excess and their total amount was kept constant at 150 μmol in all experiments. The solutions were kept for ~15 h to complete ligand exchange. The precipitate of thiol-coated MC Au NPs was allowed to settle down, the

mother-liqueur was decanted, and the solid was washed with CH_2Cl_2 (3×30 ml) and acetone (1 × 30 ml). Finally, all precipitates of mSAM-coated Au NPs were dried and dissolved in 10 ml of water to obtain ~15 mM solutions of NPs. The pH of the solutions was adjusted to ~11 with 0.2 M solution of NMe_4OH.

c. Crystallization. In a typical procedure, solutions of mixed-charged NPs (2-3 μmols) were prepared at two different pH values (~ 4 and ~11) in a 2:1 v/v mixture of water and anhydrous dimethyl sulfoxide (DMSO), and crystals were grown by slow (over ~ 36 h) evaporation of water at 65° C. Afterwards, DMSO was decanted and the precipitate washed several times with acetonitrile to remove excess salts. The mixture of crystals was then analyzed by TEM and SEM microscopies and small angle X-ray diffraction.

d. Zeta potential measurements. The electrophoretic mobility of NPs was measured with Zeta/PALS particle sizer and surface potential analyzer (Malvern Instruments). The zeta potentials were derived from electrophoretic mobility values using Hückel approximation.

e. NMR studies. Before NMR experiments, the Au cores of the NPs were etched using molecular I_2, following the procedure of Murray and co-workers.[S2] Excess of I_2 was removed by washing with methanol and drying at 65 °C to remove the solvent. Subsequently, the thiol mixtures were dried under vacuum for 15 h to remove traces of water and methanol. The purified thiol mixtures were dissolved in deuterated DMSO and ^1H NMR spectra were taken on a 500 MHz Inova apparatus. A typical spectrum of MUA/TMA thiol solution (α_{surf} = 1.6) in d^6-DMSO is shown in Fig. S1. The composition of the mixture was estimated from the integrals of peaks originating from methylene groups attached to the trimethylammonium group of the TMA thiol ($R\text{-}CH_2\text{-}NMe_3^+Cl^-$, σ ~ 3.28 ppm) and the methylene group next to the carboxylic group of MUA thiol ($R\text{-}CH_2\text{-}COOH$, σ ~ 2.17 ppm). Note: These studies required large quantities of particles. The amounts of NPs used to obtain each spectrum corresponded to at least 1 mg of thiol.

f. SAXS measurements. A drop of concentrated NP crystals was dried on krypton tape and the diffraction pattern was measured on a Rigaku S-MAX 3000 High Brilliance SAXS-WAXS System with a Cu Kα MicroMax source and a Fuji image plate collecting the WAXS-GIWAXS pattern. The Q-range was 0.01 to $1Å^{-1}$.

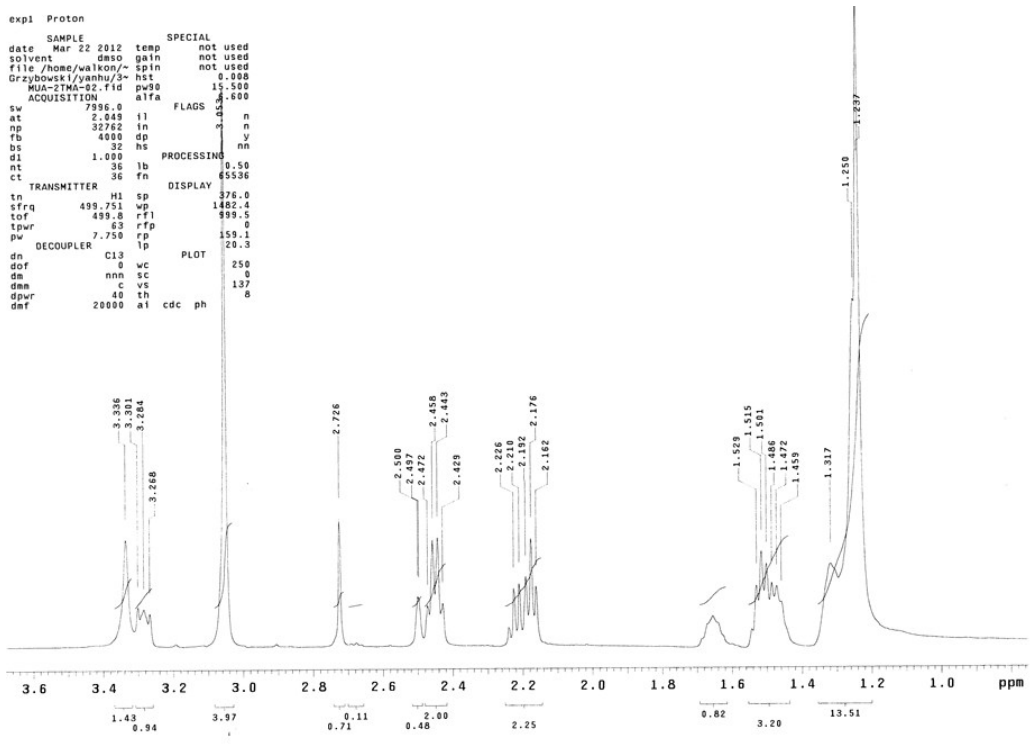

Fig.S1 ^{1}H NMR spectrum of MUA/TMA ligands (α = 1.6) in d^6-DMSO after etching the Au NP cores (adapted from ref. 3. Copyright 2013 American Chemical Society).

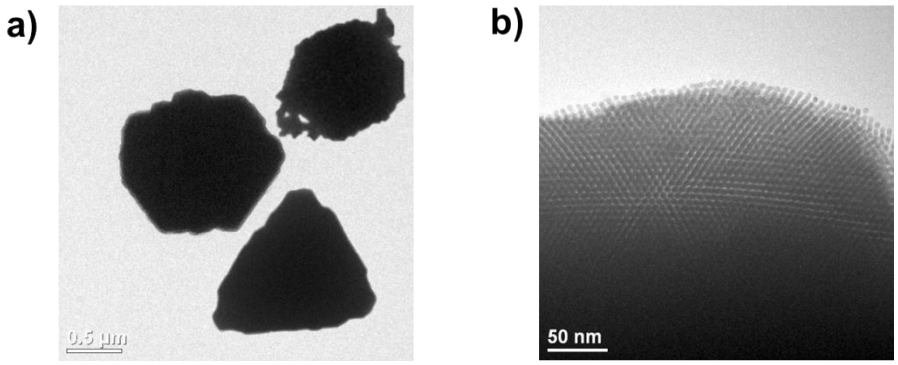

Fig. S2 TEM images of 3D crystals obtained from the self-assembly of 5.5 nm Au NPs (α = 1.6) at pH ~ 4, at two different magnifications. Individual NPs can be seen in the high magnification image (**b**).

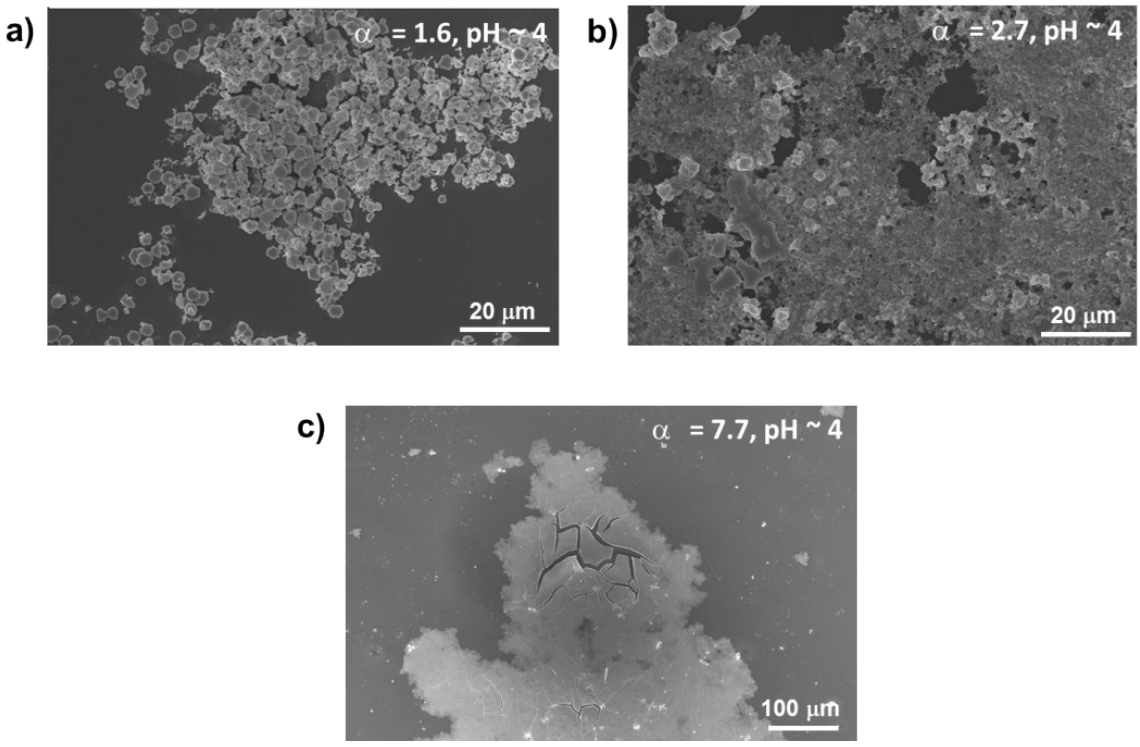

Fig. S3 Effect of surface composition on crystal formation. SEM images of (a) regularly faceted crystals obtained from α = 1.6 NPs, (b) random non-crystalline aggregates obtained from α = 2.5 MC NPs, and (c) a film of a NP precipitate obtained from α = 7.7 MC NPs.

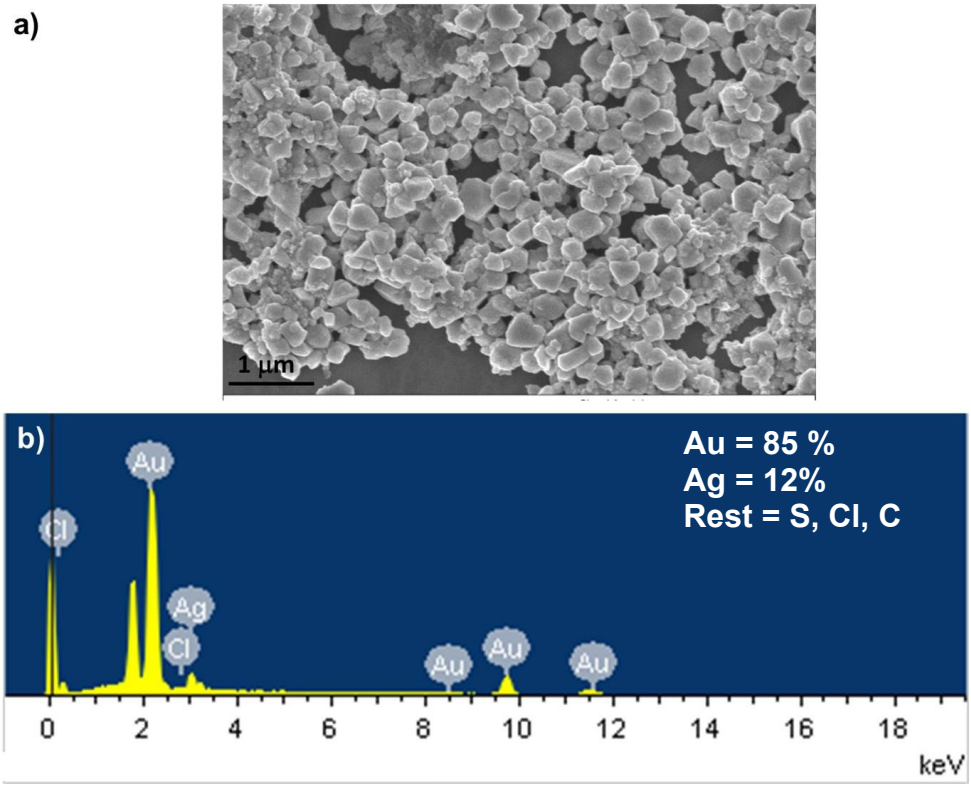

Fig. S4 (**a**) Large area SEM image and (**b**) EDX spectrum of crystals formed from the self-assembly of 5.5 nm MUA/TMA AuNPs (α = 1.6) and 6 nm TMA AgNPs at pH ~ 4.

a)

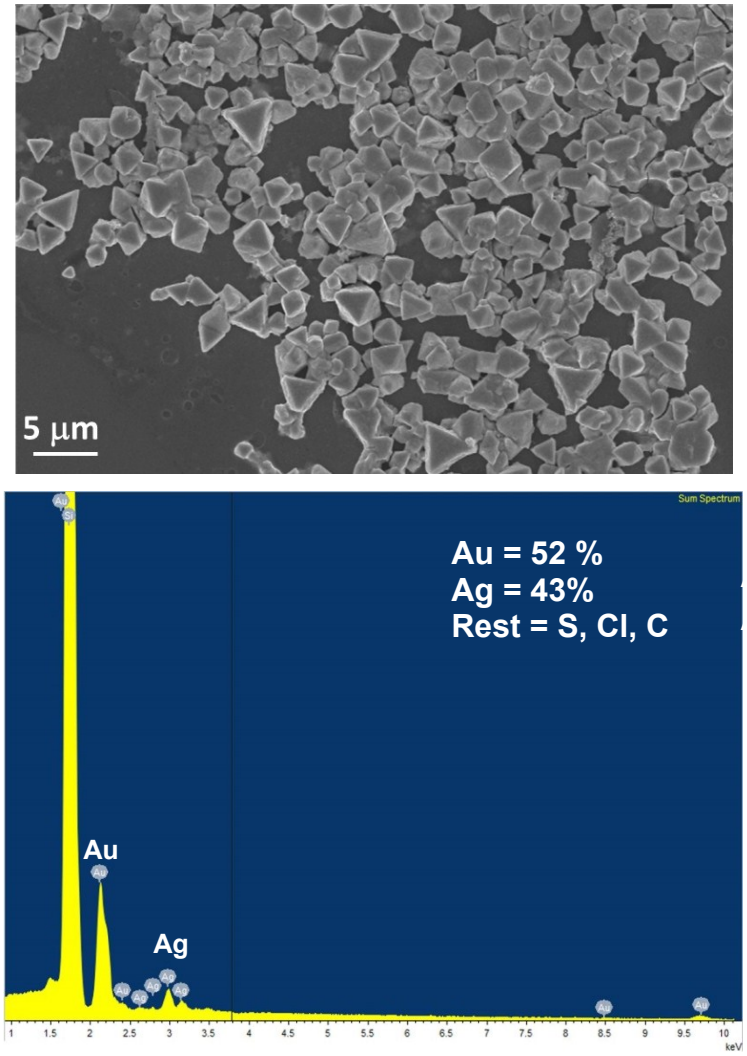

Fig. S5 (**a**) Large area SEM image and (**b**) EDX spectrum of binary crystals formed from the self-assembly of 5.5 nm MUA/TMA AuNPs (α = 1.6) and 6 nm TMA AgNPs at pH ~ 11.

Effect of Temperature on Interparticle Forces

As narrated in the main text, the NPs were crystallized at ~ 65 ^{0}C to slowly evaporate water from the water/DMSO mixture. This choice of temperature provided the "best compromise" between very slow evaporation at lower temperatures and desorption of the thiol ligands from the NPs at higher temperatures (effectively destroying the NPs). In other words, the range of temperatures this system admits is quite narrow. Still, anticipating that more thermally stable ligand shells might be used in other systems, we provide here a brief summary of the temperature scaling of interparticle forces acting in the system – that is, of the van der Waals, electrostatic, and H-bonding interactions.

1. van der Waals forces have three major contributions[S4]:

1.1. Keesom or dipole-dipole interactions: The average energy between two permanent dipoles separated by distance *r* is given by $U = -\frac{2\mu_1^2\mu_2^2}{3(4\pi\varepsilon_0)^2 r^6 k_B T}$, where μ_1, μ_2 are dipole moments, ε_0 is the permittivity of the free space or vacuum, k_B is the Boltzmann constant, and T is temperature. The negative sign in the equation means that this interaction is attractive. Importantly, it scales inversely with temperature, $U \propto 1/T$, as greater thermal motion at higher temperature overcomes the orienting effect of the interacting dipoles.

1.2. Debye or dipole-induced dipole interactions: The average interaction between a dipole and a polarizable object is given by $U = -\frac{\mu_1^2 \alpha_2^{'}}{(4\pi\varepsilon_0) r^6}$, where μ_1 is the permanent dipole moment, $\alpha_2^{'}$ is the polarizability volume, and r is the distance between the two dipoles. These interactions are independent of temperature.

1.3 London forces or induced dipole- induced dipole interactions: The average interaction between two polarizable objects is given by $U = -\frac{3}{2}\alpha_1^{'}\alpha_2^{'}\frac{I_1 I_2}{(I_1 + I_2) r^6}$, where $\alpha_1^{'}, \alpha_2^{'}$ are the polarizability volumes, I_1, I_2 are the ionization energies, and r is the distance between the two dipoles. These interactions are independent of temperature.

2. Electrostatic interactions: The electrostatic potential around NPs is well approximated by the linearized Poisson-Boltzman equation,[S5,S6] $\nabla^2 = \kappa^2 \varphi$, where $\kappa^{-1} = \left(\frac{\varepsilon_0 \varepsilon k_B T}{2 c_s e^2}\right)^{1/2}$ or $\kappa \propto \frac{1}{\sqrt{T}}$. In this equation, κ^{-1} is the screening length, φ is the electrostatic potential, $\varepsilon_0, \varepsilon$ are the permittivity of free space and of the medium, respectively, e is the elementary charge, and c_s is the molar concentration of the electrolyte. For spherical double layers, the above

equation can be solved to give [S6] $\varphi = \varphi_0\left(\frac{R_s}{r}\right)exp(-\kappa(r - R_s))$ or $\varphi \propto exp\left(\frac{-1}{\sqrt{T}}\right)$, where R_s is the radius of a spherical particle, and r is the distance of any point in the double layer from the center of the particle. In other words, the strength of the electrostatic interaction (in our system, repulsive) increases with increasing temperature (this is so because of thedesorption of counterions and increase in the screening length).

3. Hydrogen bonding interactions: As H-bonding interaction depends on the orientation of molecules, an increase in temperature will offset the orientations thereby decreasing the strengths/number of H-bonds; the increase in temperature manifests itself by the increase of the distances between atoms participating in H-bond formation [S7].

Based on the above discussion, a qualitative graph of the variation of the relevant forces with temperature can be plotted as below. As seen, even if one could increase the temperature without desorbing the ligands from NP surfaces, the weakening vdW interactions combined with increasing electrostatic repulsion of our like-charged NPs would have prevented the assembly of such particles into crystals.

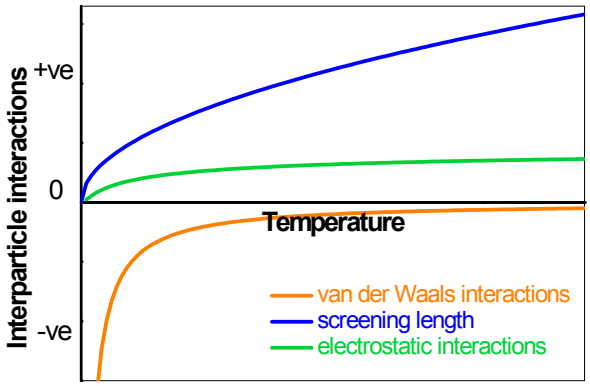

Fig. S6. A qualitative plot illustrating the scaling of the van der Waals and electrostatic interactions with temperature.

Supplementary References:-

S1. N. R. Jana, Peng, X. G, *J. Am. Chem. Soc.* 2003, **125**, 14280.

S2. M. J. Hostetler, A. C. Templeton, R.W. Murray, *Langmuir* 1999, **15**, 3782.

S3. P. P. Pillai, S. Huda, B. Kowalczyk, B. A. Grzybowski, *J. Am. Chem. Soc.* 2013, **135**, 6392.

S4. P. Atknis and J. D. Paula *Atkin's Physical Chemistry*, Oxford University Press, Ninth Edition, 2011, pp 631-637.

S5. K. J. M. Bishop, C. E. Wilmer, S. Soh and B. A. Grzybowski, *Small* 2009, ***5***, 1600–1630.

S6. K. J. M. Bishop, B. Kowalczyk and B. A. Grzybowski, *J. Phys. Chem. B* 2009, **113**, 1413–1417.

S7. A. Rastogi, A. K. Ghosh and S. J. Suresh, Hydrogen bond interactions between water molecules in bulk liquid, near electrode surfaces and around ions, *In Thermodynamics - Physical Chemistry of Aqueous Systems*, J. C. Moreno-Piraján (Ed.) InTech, **2011**, pp 351-364.